www.vbripress.com/aml, DOI: 10.5185/amlett.2016.6014 Published online by the VBRI Press in 2016

Titanium dioxide nanotube arrays: A novel approach into periodontal tissue regeneration on the surface of titanium implants

S. Goodarzi[1*], F. Moztarzadeh[1], N. Nezafati[2], H. Omidvar[3]

[1]*Biomaterials Group, Faculty of Biomedical Engineering (Center of Excellence), Amirkabir University of Technology, P.O. Box 15875-4413, Tehran, Iran*

[2]*Bioengineering Research Group, Nanotechnology and Advanced Materials Department, Materials and Energy Research Center (MERC), P.O. Box 14155-4777, Tehran, Iran*

[3]*Materials science Group, Faculty of Mining and Metallurgical Engineering, Amirkabir University of Technology, P.O. Box 15875-4413, Tehran, Iran*

[*]Corresponding author. E-mail: Saba.goodarzi@gmail.com

Received: 08 June 2015, Revised: 07 December 2015 and Accepted: 10 January 2016

ABSTRACT

Titanium alloys have been extensively used as promising implant materials. The anodic oxide layer on the surface of this alloy can be a compact, porous or a tubular structure, which has a direct impact on the final characteristics of the implants. In this study, nano topographic oxide arrays were synthesized on the surface of titanium substrates using an anodic oxidation technique. The anodization process was performed at a two-electrode electrochemical cell, and then the samples were annealed to obtain crystalline structures. The synthesized samples were analyzed to evaluate the compositional phase, morphology, surface hydrophilicity and corrosion resistance of the nanostructured oxide arrays in artificial saliva. Microscopic observations confirmed the formation of a nanotubular structure on the surface of titanium substrate depending on the anodization condition. After heat-treatment at 570 °C, crystallographic analyses showed that the obtained crystalline phase was a mixture of Anatase and Rutile phases. The electrochemical impedance spectroscopy (EIS) results indicated a significant improvement in the corrosion resistance and electrochemical stability of the anodized sample in artificial saliva compare to the control samples. In addition, the anodized samples showed a better hydrophilic characteristics, viability and proliferation of periodontal ligament cells in comparison with the un-anodized samples. This study demonstrated that the anodized titanium samples, with the nanotubular structure on the surfaces, could be considered as a good candidate for dental implants.

Keywords: Titanium dioxide nanotube; anodization; hydrophilicity; artificial saliva; periodontal ligament cells.

Introduction

Titanium and its alloys have been extensively used for dental implant root in dentistry because of their favorable mechanical properties, corrosion resistance and admirable biocompatibility [**1-3**]. In recent years, different approaches towards development of dental implants have been emerged that include changes in shape and design of implants, improvement of surface topography and fabrication of nanostructure coating in order to promote dental implant osseointegration [**4**]. Osseointegration has been considered as an optimal condition for implant and alveolar bone interface since current dental implants have a direct contact with bone meanwhile in natural teeth, periodontal ligament tissue exists between teeth's root and mandible bone. This difference has made some variations in biomechanical condition and mobility of implant compared with teeth [**5-8**]. Periodontal ligament consists of cells, extracellular fibers, interfibrillar, blood vessels, lymphatic vessels and nerves [**8**]. Presence of periodontal ligament around natural teeth has a great importance due to its significant functions such as tooth support, shock absorbance; anchorage of tooth in the jaw, physiological mobility during mastication. It also provides progenitor cells for alveolar bone formation and remodeling [**8-10**]. Lack of periodontal ligament around implant puts more stress on dental implant and jaw bone which results in bone loss. An alternative solution to prevent this challenge is placing periodontal ligament between bone and implant that can make forces softer [**11**].

Several surface modifications have been suggested to improve important properties such as roughness, porosity, chemical composition and crystal structure in order to encourage a close bonding interface between implants and living tissue. Thus, it is possible to convert the titanium surface into a more bioactive one [**12**]. The emergence of

nanotechnology paves the way for entering dental implantology into a new stage that provides an innovative understanding of biological process in oral cavity at nanoscale level [**13**]. Recently, nanostructures attract great attention due to their high surface-to-volume area and more biocompatibility in comparison with conventional microstructures and macrostructures. In the field of biomaterial-tissue interaction in vivo, nanoscale structure and morphological characteristics of surface play a crucial role in improvement of acceptance of implant in the body [**14, 15**]. It has been reported that cells react with biomaterial in vitro as they react in vivo, and their changes in morphology, cytoskeletal organization and proliferation is corresponding [**14-17**].

Among different nanostructures, anodized titanium dioxide nanotube arrays have revealed superior potential for biomaterial application. Many reports show that the titanium dioxide nanotube arrays would be a promising surface coating for medical implants. Corrosion behavior is one of the most important features for implant-biomaterials application. So the corrosion resistance of nanotubes should be scientifically researched before being used in surgeries [**18**]. Titanium dioxide nanotubes have been fabricated by various methods such as sol–gel, template processing, electrochemical processing, electrodeposition, and nano-imprint. Among these methods, potentiostatic anodizing of titanium foil in fluoride containing electrolytes is the most favorable technique for synthesis of self-ordered titanium dioxide nanotube arrays because of its unique advantages [**19, 20**]. Anodization is a simple, controllable and repeatable process that the thickness of oxide layer and pore diameter could be regulated [**21**]. As-synthesized nanotube structure is amorphous and additional heat treatment is needed for transforming it into anatase, rutile or brookite crystalline structure [**23**].

Anodization of titanium as a surface treatment method has been developed by Zwilling *et al.* [**22**] in chromic acid solution. Electrochemical anodization of titanium has been investigated in sulfuric acid, phosphoric acid and chromic acid with or without HF solution. Most of these studies have reached a unanimous contention that F^- is a crucial ingredient for the formation of titanium dioxide nanotubular structure, at the beginning of anodization. It also breaks down titanium dioxide layer and electrical field leads to manifestation of some pits at oxide surface. Then, F^- ions attack the pits which would transform to cylindrical nanotubular structure [**24, 25**].

Considering the significance of the presence of a soft tissue like periodontal ligament between dental implant and bone associated with its vital functions in the preservation of bone and implant, investigation of periodontal ligament cells behavior on titanium surface, especially titanium dioxide nanotube arrays (as a new coating for dental implants along with examination of its other critical properties such as roughness, wettability and corrosion resistance for implant applications) seems to be worthwhile. In this study, titanium dioxide nanotube arrays were fabricated with electrochemical anodization in acidic electrolyte, and then their surface properties and corrosion resistance were examined and compared to the un-anodized sample (titanium surface). Finally, proliferation and viability of periodontal ligament cells on the surfaces were investigated.

Experimental

Synthesis of titanium dioxide nanotube arrays

Commercially pure titanium with 0.8 mm thickness and 99.7 purity (Electrovek-steel LIc) sheet was cut into usable substrate with size around 1cm × 1cm by wire cut. Prior anodization, the sheared substrates were polished using SiC papers continual grade 400 to 1500 grit and were degreased ultrasonically in acetone and ethanol for 30 min. Then, the samples rinsed with deionized water (DI) and dried in an oven with 50 °C temperature. Immediately, the dried samples anodized in a two electrode electrochemical cell with stainless steel sheet as a cathode and Titanium foil as an anode. In this study, the anodization experiments were done in aqueous acidic solutions. The electrolyte was 200 ml deionized water containing 0.2 M H_2SO_4 (Sigma-Aldrich) and 0.2 M NH_4F (Sigma-Aldrich). All the experiments were performed at 20 V for 3h at room temperature. The current density of anodization process was recorded with a computer controlled Lutron 801 multimeter. After the anodization process, the samples were rinsed with DI water. For crystalizing the as-anodized samples, an annealing process was executed at 570 °C for 2 hrs with a heating rate of 2 °C/min.

Characterization of samples

The surface morphology and cross sectional view of the synthesized titanium dioxide nanotube arrays were characterized by a scanning electron microscope (SEM, XL30 Philips), operating at 20 kV, and measurement of nanotubes was performed by image-J software.

The crystalline phase of titanium dioxide nanotube arrays after heat-treatment was investigated by a X-Ray diffractometer (XRD, INEL Equinox 3000 France) using Cu Kα radiation (λ= 0.154187 nm) and 2θ values were between 20° and 80°. Determination of anatase- rutile ratio in titania nanotube arrays heat treated at 570 ^{0}C was accomplished with the formula which used the ratio (I_A/I_R) of the intensity of the strongest anatase reflection to the intensity of the strongest rutile reflection which in independent of fluctuation in diffractometer characteristics [**50**]. The Equation 1 was applied to calculate anatase-rutile ratio:

$$X_A = \left(1 + 1.26\frac{I_R}{I_A}\right)^{-1} \quad (1)$$

Contact angles of water droplets on the surface of un-anodized surface and titanium dioxide nanotube arrays were measured using a contact angle instrument (OCA 15 plus Data physics), in which the volume of droplets were 4 µL and Images of each water drop on the surface were taken immediately following DI water/substrate.

The 3D analysis of the surface topography and surface roughness was performed by an Atomic force microscope (AFM, Veeco, Auto probe-CP research). The scan was accomplished on each sample in intermittent contact mode

over three different places with 1.0 μm^2 area. The obtained data have been presented as mean with standard deviation from four different scan areas for anodized and un-anodized titanium.

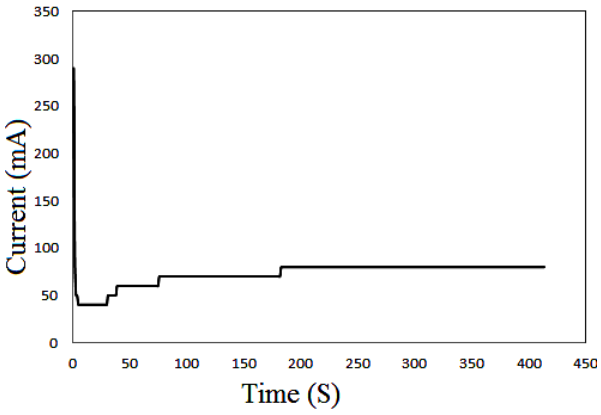

Fig. 1. Current-transient curve during anodization process of Ti foil.

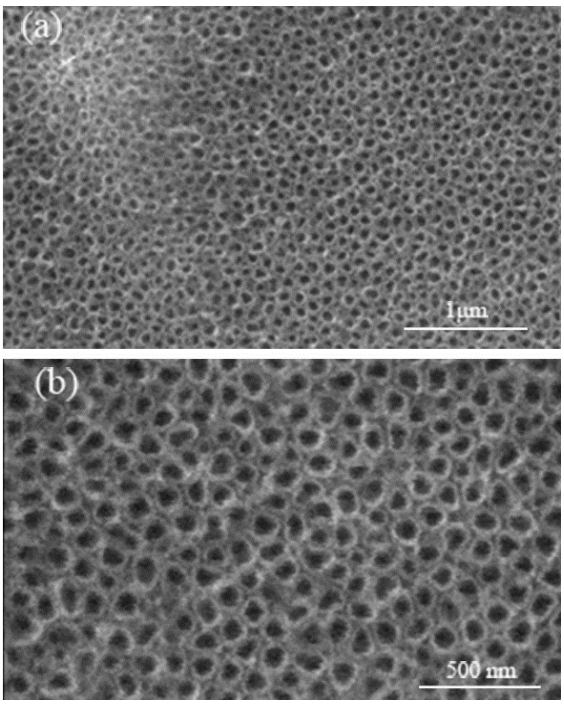

Fig. 2. SEM images of titanium dioxide nanotube arrays fabricated by electrochemical anodization a) X 20000 and b) X 40000.

The corrosion resistance of the titanium dioxide nanotube arrays was determined and compared to the un-anodized titanium sample. The electrochemical stability measurements were carried out with the IVIUMSTAT potentiostatic galvanostatic. The testing solution for electrochemical stability was an artificial saliva solution according to the composition suggested by Duffo *et al.* [**26**] by following composition: 0.6 g/l NaCl, 0.72 g/l KCl, 0.22 g/l $CaCl_2.2H_2O$, 0.68 g/l KH_2PO_4, 0.856 g/l $Na_2HPO_4.12H_2O$, 0.06 g/l KSCN (Potassium thiocyanate), 1.5 g/l $KHCO_3$, 0.03 g/l Citric acid and adjusted to pH value of 6.5. All the chemical ingredients were purchased from Merck chemicals. The titanium samples with an exposed surface area of 1 cm^2 were used as the working electrode. The impedance spectra were acquired in the frequency range of 10 mHz to 100 kHz and with 0.001 V/S scanning rate. The obtained data from EIS experiments were analyzed and fitted by Iviumsoft software.

Periodontal ligament cellular evaluation

Cell culture**:** The periodontal ligament cells were attained from periodontal ligament tissues of freshly extracted bicuspid root surfaces in a 28 years old female donor and isolated based on an Institutional Review Board approved protocol from teeth root. The extracted teeth were rinsed with PBS containing penicillin, amphotericin and gentamycin. The obtained periodontal ligament tissues were washed and cells were cultured Dulbecco's modified Eagle's medium containing 10 % fetal calf serum supplemented with 2 mM L-glutamine, 100 IU ml^{-1} of penicillin, and 100 µg ml^{-1} of streptomycin.

Cell morphology**:** Initially, the sterilized samples were placed in the wells of a 24 wells plate, and then 10000 - 15000 cells with a volume of 100 µL were added to each sample in the wells. After 5 hr incubation and adhesion of the cells, the culture medium containing 10 % FBS was added to each well. After 2 days, the culture medium was removed and the periodontal ligament cells were fixed with glutaraldehyde to study their morphology on the anodized nanotube and titanium control surfaces by a scanning electron microscope (SEM, Seron AIS2100).

Cell proliferation**:** One of the best indirect methods in order to determine cell proliferation is 3-[4, 5-dimethylthiazol-2yl]-2, 5-diphenyl tetrazolium bromide (MTT) assay that was used here to evaluate the proliferation rate of human periodontal ligament on the samples. For this purpose, 3×10^3 cells with 100 µL culture media were added to each sample in a 24 wells plate, after 4h of incubation at 37 °C 1 mL, the culture media was added to each well and distinctive amount of culture media was added to wells at regular intervals.

After 5 and 10 days, the culture media was removed from each sample and 300 µL MTT with 0.5 $mg.mL^{-1}$ concentration was added to each well and they were placed in an incubator for 4h. Then, 300 µL isopropanol was added to them and solution was transferred to a 96 wells plate. The optical density of the solution in each well was measured at wavelength of 545 nm using an Elisa plate reader (STAT FAX 2100, USA). The collected data have been presented as mean with standard deviation from four different samples for each anodized and control sample and the cell viability percent was determined relative to control sample (un-treated titanium).

Results and discussion

Current-transient curve during anodization of Titanium foil which demonstrated current-time behavior in anodization process performed at the constant voltage of 20 V is shown in **Fig. 1**. The morphology of the titanium dioxide nanotube arrays produced with electrochemical anodization in two different magnifications is shown in **Fig. 2**. It is obvious that the entire surface of the titanium samples were covered with this nanostructured pattern. The pore diameter and wall thickness of the nanotubes, which was measured by

Image J software, were 120±3 nm and 20±3 nm, respectively. The **Fig. 3** also represents the cross sectional view of TiO_2 nanotubes, while the overall length of nanotubes was estimated about 774±3 nm.

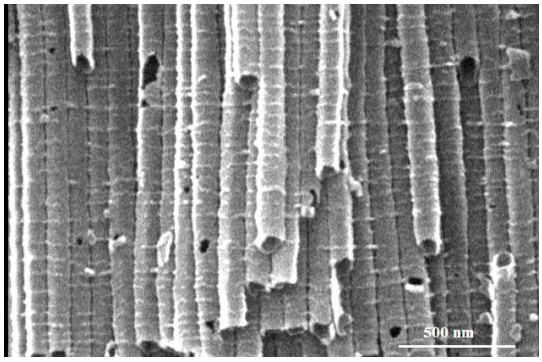

Fig. 3. SEM image of cross sectional view of TiO_2 naotube arrays fabricated by electrochemical anodization.

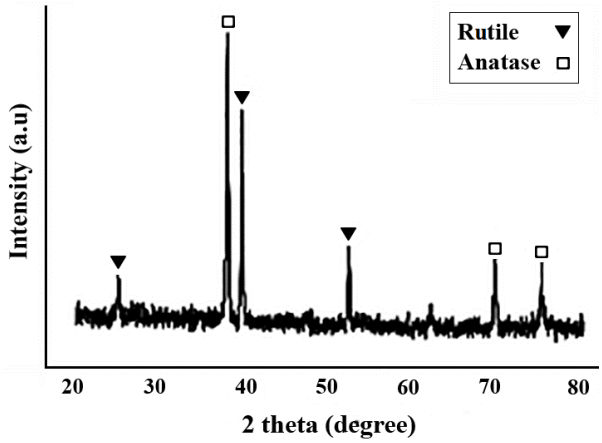

Fig. 4. XRD pattern of titanium dioxide nanotube arrays after heat-treatment at 570 ºC for 2h.

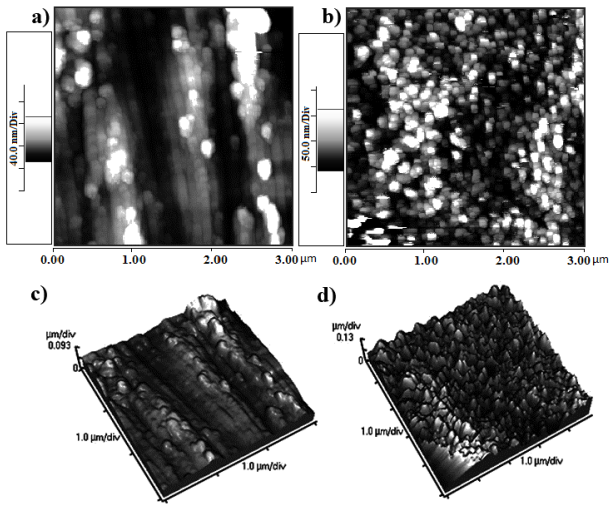

Fig. 5. a) and b) 2D, and c) and d) 3D AFM images for the un-treated titanium and titanium dioxide nanotube arrays, respectively.

Fig. 4 shows the XRD pattern of the heat-treated sample. As can be seen, the as-formed titanium dioxide nanotubes typically have an amorphous structure. Numerous studies have shown that titanium dioxide nanotubes could be transformed to anatase phase or a mixture of anatase and rutile at temperatures higher than 280 °C and 450 °C in air, respectively [**27-31**]. In particular, the titanium dioxide nanotube anatase polycrystalline phase is known to play an important role in cell proliferation and morphology [**34**]. Based on previous studies, a combination of anatase and rutile phases led superior cellular activities [**32, 33**], so nanotubes were heat-treated at 570 °C to obtain anatase-rutile structures, as shown in **Fig. 4**. As described in experimental section the weight fraction of anatase and rutile phases based upon XRD results is 50.35 % and 49.64 %, respectively, which was calculated with equation 1.

Cell adhesion is an essential procedure that can lead to further cell behavior such as cell growth, migration and differentiation. It is known that surface properties of biomaterials can greatly influence the cell-biomaterial interactions. One of the most important surface properties of implants is surface roughness and topography which directly affects cellular behavior [**35**] especially roughness values on nano scales perform a significant role in the adsorption and adhesion of proteins and cells [**36**]. Three dimensional AFM images for both un-anodized titanium and titanium dioxide nanotubes are shown in **Fig. 5**. As it could be found from AFM images, titanium dioxide nanotube arrays has generated an almost uniform rough surface on titanium and has increased its surface roughness. The root mean square parameter (rms) and roughness average (R_a) for the un-treated titanium and titanium dioxide nanotube arrays have been measured and shown in **Table 1**.

Table 1. Quantitative data obtained by AFM analysis for un-anodized titanium surface and titanium dioxide nanotube arrays.

Sample	Root-mean-square roughness (nm)	Average roughness (nm)
Un-anodized titanium	19.79±0.52	14.55±0.98
Titanium dioxide nanotube arrays	35.01±0.88	26.95±0.83

These values for titanium dioxide nanotube arrays in comparison with the un-treated titanium were much higher and have represented higher roughness of nanotube coating. Despite of these different values, the difference in the surface roughness was not noteworthy, and this might be related to the surface preparation of samples which affected this parameter.

The surface wettability of biomaterials has been found to be an important factor for cell-biomaterial interaction, and more hydrophilic surfaces are able to improve cell attachment and cellular behavior [**40, 41**]. This property can affect cell-biomaterial interaction, since the culture media is a water based liquid and in hydrophobic surfaces, poor cell attachment could be observed [**42**]. Contact angle measurements were conducted to investigate the surface wettability of the samples by determining the degree of phase separation instantly following deionized water (DI)/substrate contact. The shape of water drops on the titanium and titanium dioxide nanotube surfaces and the average of contact angles for the un-anodized titanium surface and the nanotube arrays have been presented in **Fig. 6**. These results showed that anodizing of titanium and fabrication of titanium dioxide nanotube arrays increased

the hydrophilicity of titanium surface, resulting in an improvement in the cell-implant interaction. This might be because of the increase in the surface roughness, as abovementioned. The surface wettability of the nanotube structures can be changed by roughening titanium surface. The formation of nanotube arrays on the titanium substrate alters its surface from hydrophobic to hydrophilic because the nanotubular structure lets the liquid penetrate deeper into the film and results in decreasing the contact angle [**37-39**].

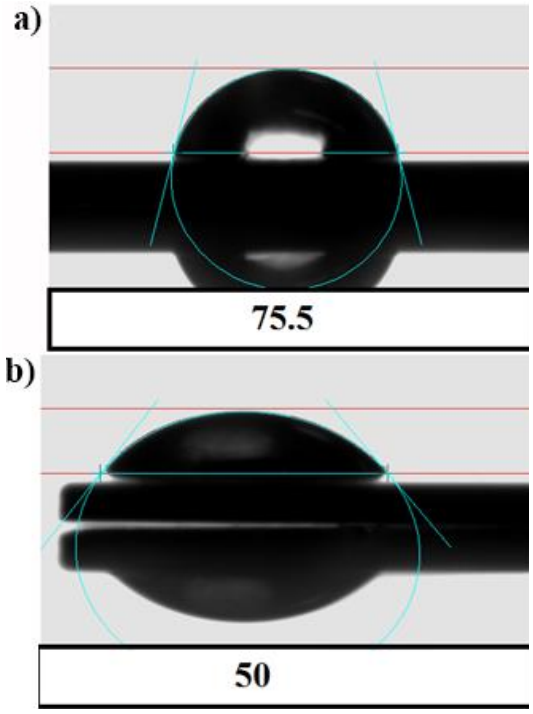

Fig. 6. Contact angle experiments for a) the un-treated titanium and b) titanium dioxide nanotube arrays.

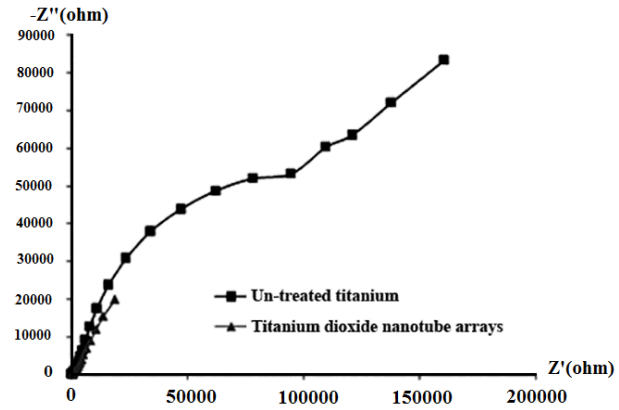

Fig. 7. Nyquist diagram for the un-treated titanium and titanium dioxide nanotube arrays.

Potentiostatic EIS is a perturbative characterization technique of an electrochemical process that uses to characterize an electrochemical interface and to study the corrosion behavior of coated metals. The EIS data could provide useful information about the properties of passive films [**44, 45**]. The heat-treated titanium dioxide nanotubes were examined by electrochemical impedance spectroscopy to investigate their corrosion behavior in artificial saliva and to compare coated titanium with bare and mechanically polished titanium. Nyquist and Bode plots of EIS data have been shown in **Fig. 7** and **Fig. 8**, respectively. The impedance spectra data are fitted with Iviumsoft software and interpreted with equivalent circuits, have been also shown in **Fig. 9**.

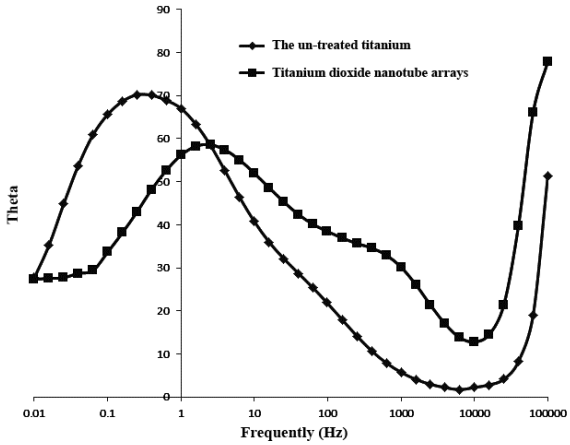

Fig. 8. Bode diagram for the un-treated titanium and titanium dioxide nanotube arrays.

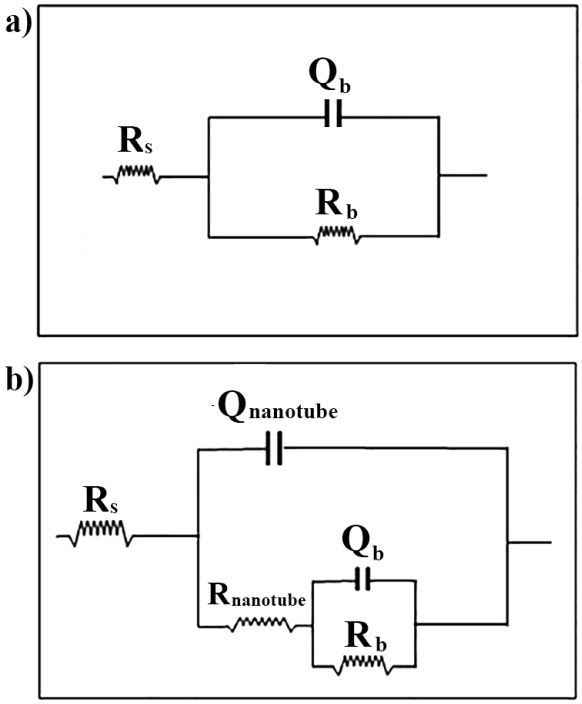

Fig. 9. Equivalent circuits used to fit impedance diagrams, a) the un-treated titanium, and b) the anodized titanium.

Nyquist diagram of the un-anodized titanium sample has exhibited one semicircle while corresponding diagram for titanium dioxide nanotube arrays has shown two semicircles. This difference is related to the presence of two layers in the anodized titanium coating, i.e.: nanotubular layer and barrier layer. In addition, the size of semi-circle arc is related to oxide layer stability. The results of electrochemical impedance spectroscopy have been also shown according to Bode diagram (**Fig. 8**). For the titanium dioxide nanotube arrays, the presence of two time constants in Bode diagram confirmed the existence of two layers in

the titanium dioxide nanotube structure meanwhile the bare titanium sample illustrated just one time constant.

Two equivalent circuits which correspond to the bare titanium and nanotube coated titanium are shown in **Fig. 9**, where R_s is solution resistance, R_b is charge transfer resistance, Q_b is constant phase element of barrier layer; $R_{nanotube}$ is porous oxide resistance and $Q_{nanotube}$ is constant phase element related to the porous layer.

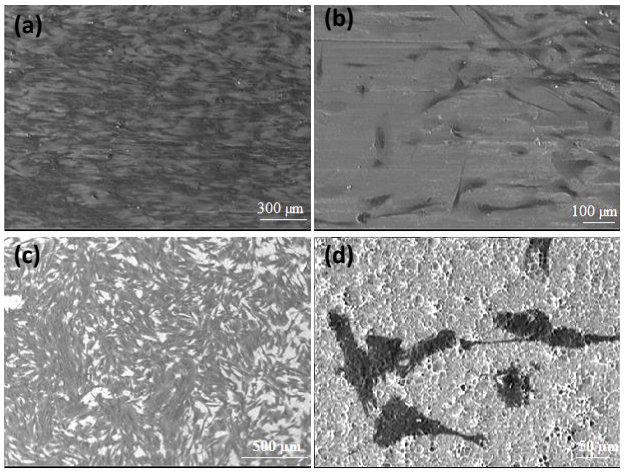

Fig. 10. Low and high magnification SEM images of periodontal ligament cells after two days of culture on: a) and b) the un-treated titanium, c) and d) the anodized titanium, respectively.

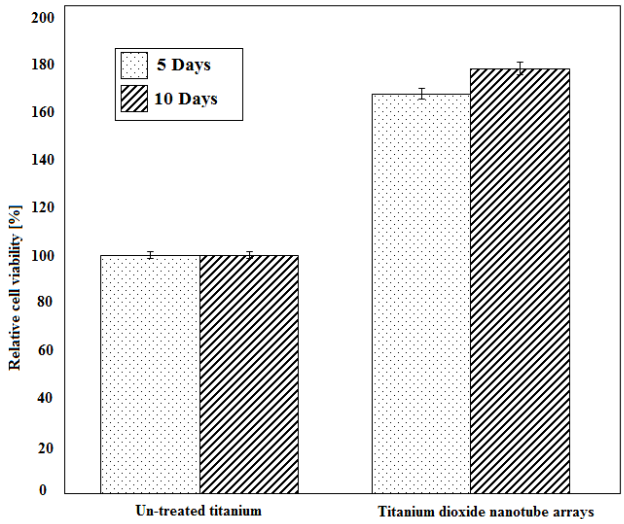

Fig. 11. Relative cell viability of periodontal ligament cells after 5 and 10 days of cell culture in contact with the un-treated titanium and titanium dioxide nanotube arrays based on MTT assay results (Values are expressed as mean ± S.E.M. of four experiments.).

The constant phase element (CPE) was used to describe the frequency independent shift between the AC potential and its current response. The electrical parameters obtained by fitting equivalent circuits are shown in **Table 2**. As mentioned above, the electrochemical experiments have been accomplished in artificial saliva in order to demonstrate the stability of the titanium dioxide nanotube coating and its corrosion resistance for dental implant applications. The higher resistance in equivalent circuits corresponds to higher corrosion resistance and electrochemical stability for the titanium dioxide nanotube coating. The amount of electrical parameters in circuits has demonstrated that the electrochemical stability of the titanium dioxide nanotube layer corresponds to the barrier layer is higher than porous layer.

Table 2. Impedance component for un-anodized titanium surface and titanium dioxide nanotube arrays.

Electrical parameters	$R_s(\Omega)$	$R_b(\Omega)$	$Q_b(\mu F)$	$R_{nanotube}(\Omega)$	$Q_{nanotube}(\mu F)$
Un-anodized titanium	725	1.6×10^4	$2.55e^{-5}$	--------	--------
Titanium dioxide nanotube arrays	375	2.4×10^5	0.599	10190	0.585

The major difference between natural teeth and conventional dental implants is the presence of periodontal ligament tissues interposing tooth root and alveolar bone while this tissue is not present when natural tooth replaced with an implant. A large number of studies have proven the significant functions of periodontal ligament tissues in the absorbance of shocks, prevention of plaque accumulation, spreading of inflammation around teeth and also providing alveolar bone with progenitor osteoblast cells [**11, 46**]. As it was mentioned above, investigation of periodontal ligament cells is very important. In this way, one of the most momentous steps in establishing hemostasis condition at biomaterial-tissue interface is cell attachment. Cell attachment is a fundamental factor for matrix synthesis, cellular differentiation, integration and finally healing process around an implant [**47, 48**], accordingly, surface characteristics of implants is the most influential factor on cell-biomaterial interaction at their interface [**35**]. Many experiments have been carried out to establish periodontal ligament tissues around dental implants, since periodontal ligament cells possess ability to reestablish connective tissue attachment [**49**]. In this study, cells proliferation and viability studies have been carried out by MTT assay experiment and cells attachment, and their morphology were observed with an SEM. **Fig. 10** represents SEM images of periodontal ligament cells after two days of culture that have been fixed on different samples. The comparison between the cells morphology on the titanium surface and titanium dioxide nanotube coatings reveals that the titanium dioxide nanotube arrays supply more suitable conditions for periodontal ligament cells, since cells spread on the nanotube structure more efficiently. In fact, there is a noticeable difference between cell morphology on the un-treated titanium and titanium dioxide nanotube arrays. As can be seen, filopedia propagation on the titanium surface is less than titanium dioxide nanotube coating and periodontal ligament cells are more elongated on the nanotubes because of better interaction of cells with nanotubes. However the morphology of nanotubes is not completely clear in Figure 10, since the surface of titania nanotubes is covered by fixation materials to some extent.

After initial stage of cell-biomaterial interaction and consequently, cell attachment, it is essential to examine cell viability and proliferation that have been done by MTT assay at 5 and 10 days of cell culture on the surfaces of substrates. The results of MTT assay were shown in **Fig. 11**. As it can be seen, there is significant difference between flat titanium as the control sample and titanium dioxide nanotube coating after various days of cell culture. The increase in the amount of cell viability with the passage

of time reveals the fact that although titanium is biocompatible biomaterial for periodontal ligament cells, fabrication of titanium dioxide nanotube arrays as a porous oxide coating augments the biocompatibility of titanium dental implants extensively and increases number of viable cells on implant surface noticeably.

Conclusion

In this study, titanium dioxide nanotube arrays were fabricated through an anodization process in an acidic solution containing H_3PO_4 and NH_4F, subsequently, and then heat-treated in order to obtain a crystalline structure. According to the obtained results, the characteristics of the anodized titanium surfaces were enhanced extensively in comparison with the bare titanium surfaces, such as wettability, roughness and corrosion resistance. To examine the biocompatibility of the samples, the viability and attachment of periodontal cells were tested on the surface of the samples. It was shown that the titanium dioxide nanotubes exhibited a better cell adhesion and spreading, and more anchorage sites were observed for filopedia propagation when compared to the pure titanium samples. In addition, MTT assay represented that there was a considerable difference in the viability and proliferation of periodontal ligament cells on the surface of bare titanium and titanium dioxide nanotube structure. It was demonstrated that the synthesized titanium dioxide nanotube arrays were more biocompatible than the polished titanium. This study showed that the nanotubular structure on the surface of titanium substrate could make it a promising candidate for applications such as dental implants.

Reference

1. Hamadaa, K.; Kon, M.; Hanawa, T.; Yokoyama, K.; Miyamotoc, Y. Asaoka, K., *Biomaterials* **2002**, *23*, 2265.
2. Diamanti, M. V.; Ormellese, M.; Pedeferri, M., *Corrosion Science* **2010,** *52*, 1824.
3. Dey, T.; Roy, P.; Fabry, B.; Schmuki, P., *Acta Biomaterialia*, **2011**, *7*, 1873
4. Lin, Y.; Gallucci, G. O.; Buser, D.; Bosshardt, D.; Belser, U. C.; Yelick, P. C., *J Dent Res*, **2011**, *90*, 251.
5. Marei, M. K.; Saad, M. M.; El-Ashwah, A. M.; El-Backly, R. M.; Al-Khodary, M. A. *J. Oral Implantol* **2009**, *35*, 106.
6. Lin, C.; Dong, Q. S.; Wanga, L.; Zhang, J. R.; Wu, L. A.; Liu, B. L., *Medical Hypotheses*, **2009**, *72*, 58.
7. Kado, T.; Hidaka, T.; Aita, H.; Endo, K.; Furuichi, Y., *Applied Surface Science*, **2012**, *262*, 240.
8. Kano, T.; Yamamoto, R.; Miyashita, A.; Komatsu, K.; Hayakawa, T.; Sato, M.; Oida, Sh., *Journal of Hard Tissue Biology*, **2012**, *21*,189.
9. Somerman, M. J.; Archer, S.Y.; Imm, G. R.; Foster, R. A., *J Dent Res*, **1988**,*67*,66.
10. Gault, Ph.; Black, A.; Romette, J. L.; Fuente, F.; Schroeder, K.; Thillou, F.; Brune, T.; Berdal, A.; Wurtz, T., *J Clin Periodontol*, **2010**, *37*,750.
11. Kramer, Ph. R.; Janik Keith, A.; Cai, Z.; Ma, S.; Watanabe, I., *Dental Materials*, **2009**, *25*, 877.
12. Szesz, E. M.; Pereira, B. L.; Kuromoto, N. K.; Marino, C. E. B.; de Souza, G. B.; Soares, P., *Thin Solid Films*, **2013**,*528*, 163.
13. Wang, F.; Shi, L.; Xi He, W.; Han, D.; Yan, Y.; Niu, Zh. Y.; Shi, Sh. G., *Applied Surface Science*, **2013**, *265*, 480.
14. Brammer, K. S.; Oh, S.; Cobb, Ch. J.; Bjursten, L. M.; van der Heyde, H.; Jin, S., *Acta Biomaterialia*, **2009**, *5*, 3215.
15. Oh, S.; Brammer, K. S.; Li, Y. S. J.; Teng, D.; Englerb, A. J.; Chienb, Sh.; Jin, S., *Proc Natl Acad Sci, U S A.* **2009**, *106*, 2130.
16. Bjursten, L. M.; Rasmusson, L.; Oh, S.; Smith, G. C.; Brammer, K. S.; Jin, S., *J Biomed Mater Res*, **2010**, *92*, 1218.
17. Park, J.; Bauer, S.; von der Mark, K.; Schmuki, P., *Nano letters*, **2007**, *7*, 1686.
18. Yu, W. Q.; Qiu, J.; Xu, L.; Zhang, F. Q., *Biomed. Mater*., **2009**, *4*, 065012.
19. Omidvar, H.; Goodarzi, S.; Seif, A.; Azadmehr, A. R., *Superlattices and Microstructures*, **2011**, *50*, 26.
20. Tsuchiya, H.; Akakia, T.; Nakataa, J.; Terada, D.; Tsuji, N.; Koizumi, Y.; Minamino, Y.; Schmuki, P.; Fujimoto, Sh., *Electrochimica Acta*., **2009**, *54*, 5155.
21. Kim, S. E.; Lim, J. H.; Lee, S. C.; Nam, S. C.; Kang, H. G.; Choi, J., *Electrochimica Acta*, **2008**, *53*, 4846.
22. Zwilling, V.; Ceretti, E. D.; Forveille, A. B.; David, D.; Perrin, M. Y.; Aucouturier, M., *Surf. Interface Anal*, **1999**, *27*, 629.
23. Tan, A.W.; Murphy, B. P.; Ahmad, R.; Akbar, S. A., *Ceramics International*, **2012**, *38*, 4421.
24. Lockman, Z.; Sreekantan, S.; Ismail, S.; Mende, L. S.; MacManus-Driscoll, J. L., *Journal of Alloys and Compounds*, **2010**, *503*, 359.
25. Zhao, J.; Wang, X.; Chen, R.; Li, L., *Solid State Communications*, **2005**, *134*, 705.
26. Duffó, G. S.; Castillo, E. Q., *Corrosion*, **2004**, *60*, 594.
27. Varghese, O. K.; Gong, D.; Paulose, M.; Grimes, C. A.; Dickey, E. C., *J Mater Res*, **2003**, *18*, 156.
28. Macak, J. M.; Tsuchiya, H.; Ghicov, A.; Yasuda, K.; Hahn, R.; Bauer, S.; Schmuki, P., *Current Opinion in Solid State and Materials Science*, **2007**, *11*,3.
29. Oh, H. J.; Lee, J. H.; Kim, Y. J.; Suh, S. J.; Lee, J. H.; Chi, C. S., *Applied Catalysis B: Environmental*, **2008**,*84*,142.
30. Sreekantan, S.; Hazan, R.; Lockman, Z., *Thin Solid Films*, **2009**, *518*, 16.
31. Sreekantan, S.; Lockman, Z.; Hazan, R.; Tasbihi, M.; Tong, L. K.; Mohamed, A., *Journal of Alloys and Compounds*, **2009**,*485*,478.
32. Yu, W.Q.; Zhang, Y. L.; Jiang, X.Q.; Zhang, F.Q., *Oral Dis*, **2010**, *16*, 624.
33. Bai, Y.; Park, S.; Park, H. H.; Lee, M. H.; Bae, T. S.; Duncan, W.; Swain, A., *Surf. Interface Analysis*, **2011**, *43*, 998.
34. Uhm, S. H.; Song, D. H.; Kwon, J. S.; Lee, S. B.; Han, J. G.; Kim, K.M.; Kim, K. N., *Surface and Coatings Technology*, **2013**,*228*, 360.
35. Jayaraman, M.; Meyer, U.; Bühner, M.; Joos, U.; Wiesmann, H. P., *Biomaterials*, **2004**, *25*,625.
36. Brett, P. M.; Harle, J.; Salih, V.; Mihoc, R.; Olsen, I.; H Jones, F.; Tonetti, M., *Bone*, **2004**, *35*, 124.
37. Das, K.; Balla, V. K.; Bandyopadhyay, A.; Bose, S., *Scripta Materialia*, **2008**, *59*, 822.
38. Balaur, E.; Macak, J. M.; Taveira, L.; Schmuki, P., *Electrochemistry Communications*, **2005**, 1066.
39. Sobieszczyk, S., *Advances in Materials science*, **2009**, *9*, 25.
40. Stevens, M. M.; George, J., *Science*, **2005**, *310*, 1135.
41. Zhang, S., *Nat Biotech*, **2003**, *21*, 1171.
42. Das, K.; Bandyopadhyay, A.; Bose, S., *Journal of the American Ceramic Society*, **2008**, *91*, 2808.
43. Elias, C. N.; Oshida, Y.; Lima, J. H. C.; Muller, C. A., *J Mech Behav Biomed Mater*., **2008**, *3*, 234.
44. Mareci, D.; Chelariu, R.; Dan, I.; Gordin, D. M.; Gloriant, T., *Journal of Materials Science: Materials in Medicine*, **2010**,*21*,2907.
45. Balakrishnan, M.; Narayanan, R., *Thin Solid Films*, **2013**, *540*, 23.
46. Nunez, J.; Sanz-Blasco, S.; Vignoletti, F.; MuÇoz, F.; Arzate, H.; Villalobos, C.; Nunez, L.; Caffesse, R. G., *Periodont Res*, **2012**, *47*, 33.
47. Smith, B.S.; Yoriya, S.; Johnson, T.; Popat, K. C., *Acta Biomaterialia*, **2011**, *7*, 2686.
48. Bauer, S.; Park, J.; von der Mark, K.; Schmuki, P., *Acta Biomaterialia*, **2008**, *4*, 1576.
49. Gulati, M.; Anand, V.; Govila, V.; Jain, N.; Rastogi, P.; Bahuguna, R.; Anand, B., *Dental Research Journal*, **2014**,*11*, 154.
50. Spurr, Robert A.; Howard Myers., *Analytical Chemistry*, **1954**, *29*, 760.

